

# Influence of plasma nitriding on tribological performance of HVOF sprayed AISI 316L and AISI 420 stainless steel coatings

Zuleyha TASKAN , Elif OZTURK , Selman TEZCAN , Harun MINDIVAN \*

Bilecik Şeyh Edebali University, Bilecik, Turkey

\*Corresponding author: [harun.mindivan@bilecik.edu.tr](mailto:harun.mindivan@bilecik.edu.tr)

## Keywords

high velocity oxygen fuel  
low-carbon steel  
plasma nitriding  
stainless steel  
wear rate

## Abstract

Low-carbon steel has been widely used in various industrial applications and undergoes different surface treatments in contemporary practices to enhance wear resistance, corrosion resistance and hardness. Wear is a primary cause of damage to machine components under varying conditions like temperature, humidity, load and speed. This study focuses on improving wear resistance through coating applications. A reciprocal tribological test was conducted under a 30 N load with a 57.5 m sliding distance at 2500 cycles and 20 mm/s sliding speed. Two coatings, AISI 316L austenitic and AISI 420 martensitic stainless steel were applied using the HVOF method and subjected to plasma nitriding at 450 and 500 °C. Tests verified that the HVOF sprayed AISI 316L stainless steel coating nitrided at 450 °C offers the best wear resistance.

## History

Received: 08-10-2024

Revised: 14-11-2024

Accepted: 28-11-2024

## 1. Introduction

High velocity oxygen fuel (HVOF) is a thermal spray process that produces coatings with high density and low porosity. It is widely used for applying wear resistant coatings, particularly those made of stainless steel. According to ISO/WD 27307 and ASTM C633, Vencl et al. [1] looked into whether scratch testing could be used to measure the adhesion and cohesive strength of thick plasma spray coatings. Test results from atmospheric plasma sprayed coatings showed that scratch testing could be an effective and rapid method for assessing coating cohesion. Tillmann et al. [2] evaluated the effect of mechanical pretreatments on 316L stainless steel substrates processed by selective laser melting (SLM) and their effect on the adhesion of HVOF sprayed WC-Co coatings. The research uses a stress-relief heat treatment as a reference and investigates surface roughness and residual stresses. The findings show that HVOF sprayed WC-Co coatings exhibit good adhesion to SLM 316L substrates, with the stress state affecting the WC-Co coating's adhesion more than surface

roughness. Vaz et al. [3] examined the impact of heat treatment on the properties of 316L stainless steel cold spray additives using traditional and new metal knitting strategies. Results show traditional deposition improves mechanical resistance, while metal knitting enhances part geometry accuracy. Heat treatment enhances material strength and quality. Daniel et al. [4] investigated the performance of 1.2376 high-speed steel coated with two different cobalt-based materials. They evaluated the effectiveness of the coating through impact, dry sliding, abrasive and solid particle erosion wear tests.

Thermally sprayed coatings are used for corrosion protection, wear resistance and high-temperature resistance enhancement. The performance of these coatings depends on their morphology, which includes splats, pores, oxide inclusions and unmelted particles. Vaz et al. [5] aimed to evaluate how the chemical composition of materials (carbon steel, stainless steel and FeMnCrSiNi alloy) affects the velocity, temperature and particle size of droplets. The study found that austenitic stainless steel and FeMnCrSiNi alloy increased droplet temperature during flight. Bobzin et al. [6] investigated the applicability of the impact wear test on HVOF coatings, which is



This work is licensed under a Creative Commons Attribution-NonCommercial 4.0 International (CC BY-NC 4.0) license

typically reserved for hard coatings like physical vapour deposition and chemical vapour deposition coatings. In their study, they deposited Cr<sub>3</sub>C<sub>2</sub>-NiCr on 1.0533 carbon steel using the HVOF method and conducted the impact wear test with a WC-Co ball under various cycles and loads. Their findings confirmed that the impact wear test is suitable for evaluating HVOF coatings under these conditions.

Park et al. [7] applied plasma nitriding and nitrocarburising processes to 316, 410 and 17-4 PH stainless steel at 550 °C and found that nitrocarburising outperformed plasma nitriding when evaluating HVOF sprayed stainless steel nitride layers in terms of surface hardening and layer thickness. Sagalovych et al. [8] investigated the impact of nitriding VT5 alloy (3.7115) in glow discharge plasma on its tribological characteristics in pairs with various materials in jet fuel TS-1 and under dry sliding conditions. Samples were nitrided in a nitrogen-argon gas mixture at 975 ± 15 °C and 58 ± 2 Pa. Tribological tests were performed on a friction machine 2070 SMT-1 using the "cube-roller" scheme. The results showed that the nitrided VT5 alloy had a low wear value ( $\leq 2.26 \times 10^{-6}$  mm<sup>3</sup>/Nm) and a coefficient of friction between 0.08 to 0.12. Adachi and Ueda [9] aimed to thicken the S-phase (white layer) formed by plasma nitriding on cold-sprayed 316L stainless steel coatings. They applied carburisation and nitriding processes at 400, 425 and 450 °C and investigated the effects of white layer thickness on hardness, wear resistance and corrosion resistance. Li et al. [10] performed plasma nitriding on 420 stainless steel at 440 °C with varying arc intensities, finding that increased arc intensity improved hardness, coefficient of friction, wear resistance and corrosion resistance.

Using 2.45 GHz microwave energy, Hebbale and Srinath [11] investigated the microstructure and slurry erosion wear behaviour of a cobalt-based alloy (WC-Co) coating on 420 stainless steel. The Taguchi L9 orthogonal array showed that the speed of the electric motor (1000, 1250 and 1500 rpm), the impact angle (15, 30 and 45°) and the particle size (212, 425 and 600 µm) were the most important factors affecting the wear performance. ANOVA results indicated that particle velocity is the most significant factor, followed by particle size and impact angle. The optimal settings for minimising wear were found to be 1000 rpm, 425 µm particle size and a 30° impact angle. In their study, Hussain et al. [12] examined the tribological

behaviours of UHMWPE against 316L stainless steel and Ti6Al4V biomedical implant materials under varying loading and bio-serum lubrication conditions. They analysed the friction and wear results using the Taguchi L18 orthogonal array and smaller-is-better signal-to-noise (S/N) ratio approach to identify the most significant factor and optimal condition. The ANOVA results revealed that load significantly influences wear rate and friction. They discovered that lubricating with human serum, applying a 52 N load and using Ti6Al4V as a counter-body material were the best conditions for reducing wear rate. To achieve the lowest coefficient of friction, they substitute human serum with rabbit serum in the optimal setting for wear rate.

The aim of the current study is to investigate the effects of two varying coating materials and plasma nitriding temperature on tribological performance. We statistically evaluate the specific wear rate results using a basic full factorial L4 Taguchi orthogonal array. Overall, six reciprocating tribological tests are conducted under dry sliding conditions.

## 2. Materials and methods

Initially, low-carbon steel plates were cut to dimensions 20 × 20 × 4 mm. An iron-based abrasive cutting disc was used in this cutting process. Before the spraying process, the surface of the steel plates was roughened by sandblasting and then coated with an intermediary Ni-Cr layer. This was due to the fact that the Ni-Cr layer provided an overall increase in coating thickness and corrosion resistance in conjunction with enhanced fracture toughness [13]. Figure 1 provides an example of the cross-sectional thickness variation of the Ni-Cr layer on a steel plate. Other coatings also show similar thickness values throughout the cross-section. Subsequently, the AISI 316L and AISI 420 stainless steel coatings (denoted as 316L and 420, respectively) were applied by the HVOF thermal spray process on the steel plates.

Powders used in this study were provided by Oerlikon Metco. Some physico-chemical specifications of these powders are listed in Table 1. In addition, the optimised spraying conditions are listed in Table 2. These parameters are routinely used by coating manufacturers and were originally selected to obtain high deposition efficiency.

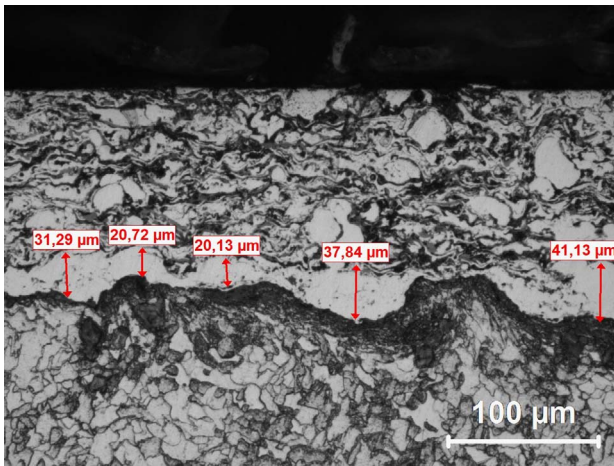


**Figure 1.** LOM image of the cross-sectional thickness variation of the Ni-Cr layer on the steel plate

**Table 1.** Properties of the used powders [14]

Powder	Stainless steel type	Size range, $\mu\text{m}$	Morphology
Diamalloy 1003	austenitic	- 45 + 11	spheroidal
Diamalloy 1002	martensitic	- 45 + 15	irregular

**Table 2.** HVOF spray parameters of 316L and 420 coatings

Parameter	Value
Flow rate of oxygen, $\text{m}^3/\text{h}$	54
Ratio of oxygen/kerosene	1.1
Carrier gas	argon
Spray distance, mm	350
Powder feed rate, g/min	70
Spray gun speed, mm/s	700

Before the plasma nitriding process, the surfaces of the HVOF sprayed 316L and 420 coatings were ground using P1200 grit size SiC paper. Ground surfaces were mechanically polished with a fine-grade  $\text{Al}_2\text{O}_3$  paste to achieve a certain surface uniformity. Finally, the surfaces were thoroughly degreased with acetone and cleaned ultrasonically.

The coatings were placed on the cathode before the plasma nitriding process and vacuumed until the process chamber pressure was 2 Pa. Hydrogen gas was then introduced into the interior until the gas pressure was 250 Pa for the "scattering process", which would provide surface cleanliness and roughness appropriate for nitriding. Scattering was carried out at 250 °C

treatment temperature for 30 minutes. After this procedure, the vacuum chamber received a fixed gas mixture of 20 %  $\text{N}_2$  and 80 %  $\text{H}_2$  for the plasma nitriding process. The process was applied at 450 and 500 °C for 12 hours in an industrial furnace. Following the completion of the nitriding process, nitrogen gas at 300 Pa was injected into the vacuum chamber and the nitrided steels were cooled to room temperature in a vacuum environment.

The nitrided steels were cross-sectioned, ground with successive SiC papers (grit size P320 – P1200) and mechanically polished at the end of the process. Samples were then etched with 2 % Nital for metallographic examinations. Table 3 lists the coating layer thicknesses for the sprayed coatings.

**Table 3.** Thicknesses of the sprayed coating layers

Coating	Plasma nitriding temperature, °C	Thickness, $\mu\text{m}$
316L	-	92.45 – 139.8
	450	89.94 – 133.2
	500	74.01 – 139.1
420	-	99.06 – 166.2
	450	90.01 – 137.6
	500	133.3 – 171.8

Microstructural characterisation of the coatings was made by microscopic examinations. Microscopic examinations were performed on the coatings' cross-sections using a Nikon Eclipse LV150 light-optical microscope (LOM). The cross-sectional microhardness measurements were carried out using a Shimadzu HVM Vickers microhardness tester with a load of 50 g and a dwell time of 15 s.

Dry sliding tribological tests of the coatings were performed on a linear reciprocating tribometer operating in a ball-on-plate configuration. An  $\text{Al}_2\text{O}_3$  ball with a diameter of 10 mm was sliding forward and backward against the coatings at a sliding speed of 1.9 cm/s. The normal load, sliding amplitude (wear track length) of the reciprocating motion and overall sliding distance of the tests were 30 N, 11.5 mm and 57.5 m, respectively. During the tribological tests, the temperature and relative humidity were maintained at  $20 \pm 5$  °C and  $40 \pm 5$  %, respectively. The tester's sensing cell automatically recorded the coefficient of friction. A surface profilometer (Mitutoyo SurfTest SJ-400) measured the width and

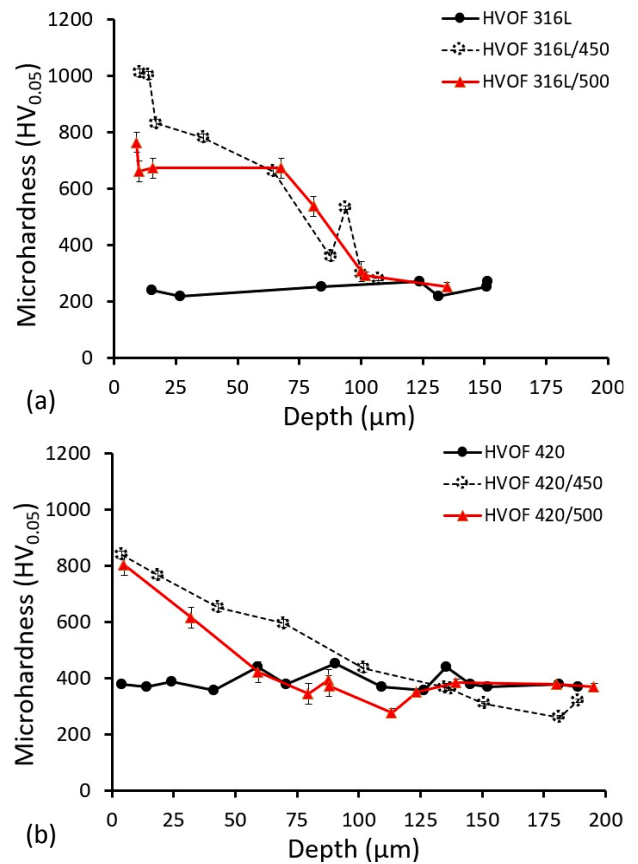
depth of the wear tracks to calculate the coatings' specific wear rate. A LOM examined the wear tracks after the tests.

### 3. Results and discussion

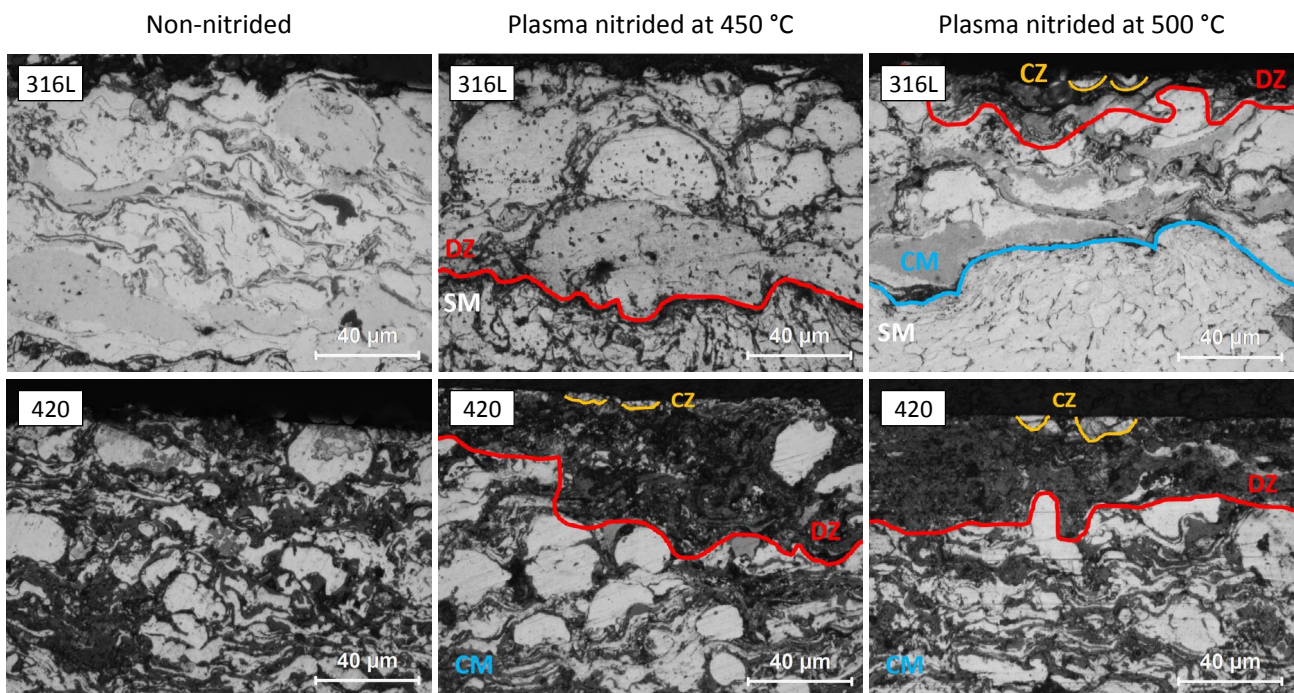
The LOM micrographs of the plasma nitrided HVOF sprayed 316L and 420 coatings can be seen in Figure 2. Since there were no separations between the coating and the substrate material, the HVOF sprayed 316L and 420 coatings formed a dense layer with strong bonding to the substrate. The coating also possessed unmelted particles, resolidified splats and oxide layers. The study found that the microstructure of both plasma nitrided HVOF sprayed 316L and 420 coatings consists of a compound zone and a diffusion zone that extends from the surface to the interior. The atomic nitrogen diffusion coefficient is reduced at lower temperatures, such as 450 and 500 °C, due to the formation of dense oxides at the splat edges in HVOF sprayed coatings, which act as barriers, resulting in thinner compound and diffusion zones similar to Mindivan [15]. It can be measured using a given scale in Figure 2 that the plasma nitrided HVOF sprayed 316L and 420 coatings have a compound zone thickness of approximately 5 μm, both at 450 and 500 °C.

Figure 3 presents the cross-sectional microhardness values of non-nitrided and plasma nitrided HVOF sprayed 316L and 420 coatings.

The hardness of non-nitrided 316L and 420 coatings is  $246 \pm 21$  HV<sub>0.05</sub> and  $388 \pm 33$  HV<sub>0.05</sub>, respectively.



**Figure 3.** Cross-sectional hardness variation of the non-nitrided and plasma nitrided HVOF sprayed coatings: (a) 316L and (b) 420



**Figure 2.** LOM images of non-nitrided and plasma nitrided HVOF sprayed 316L and 420 coatings: CZ – compound zone; DZ – diffusion zone; CM – coating material; SM – substrate material

High hardness and wear resistance requirements can be attained through surface modifications via nitriding. These attributes result from the diffusion of nitrogen into the substrate and the formation of nitrides from the metal elements that comprise the steel [16]. Nitride layers are characterised by compound and diffusion layers, exhibiting varying thicknesses based on the specific HVOF coating materials used [7]. It is clear that HVOF sprayed 316L and 420 coatings nitrided at 450 °C were harder in the top part of the diffusion zone than HVOF sprayed 316L and 420 coatings when the nitriding temperature was 500 °C.

Using the wear track width and depth values, obtained at the end of the experiment, the specific wear rates for both coatings, plasma nitrided at 450 and 500 °C, have been calculated and shown in Table 4. Corresponding wear

results in Table 4 are shown in Figure 4 in terms of the worn surface of the coating and counter-body (Al<sub>2</sub>O<sub>3</sub> ball). It is apparent that significant differences exist in the worn surfaces formed on two different coating materials treated with two plasma nitriding temperatures. The coating 316L shows shallower and narrower wear tracks than the coating 420. The coating 316L also exhibited a lower wear rate than the coating 420, which had very similar values ( $9.8 \times 10^{-5} \text{ mm}^3/\text{Nm}$ ) as shown by Mindivan and Mindivan [17]. Also, the wear tracks on the plasma nitrided HVOF sprayed coatings had oxide patches shown as red circles in Figure 4. This is a common sign of tribo-oxidation that occurs when higher test loads cause excessive friction heat [18]. The surfaces of the coatings directly correlate with the size of the wear scars on the contact surfaces of Al<sub>2</sub>O<sub>3</sub> balls, as shown in Figure 4.

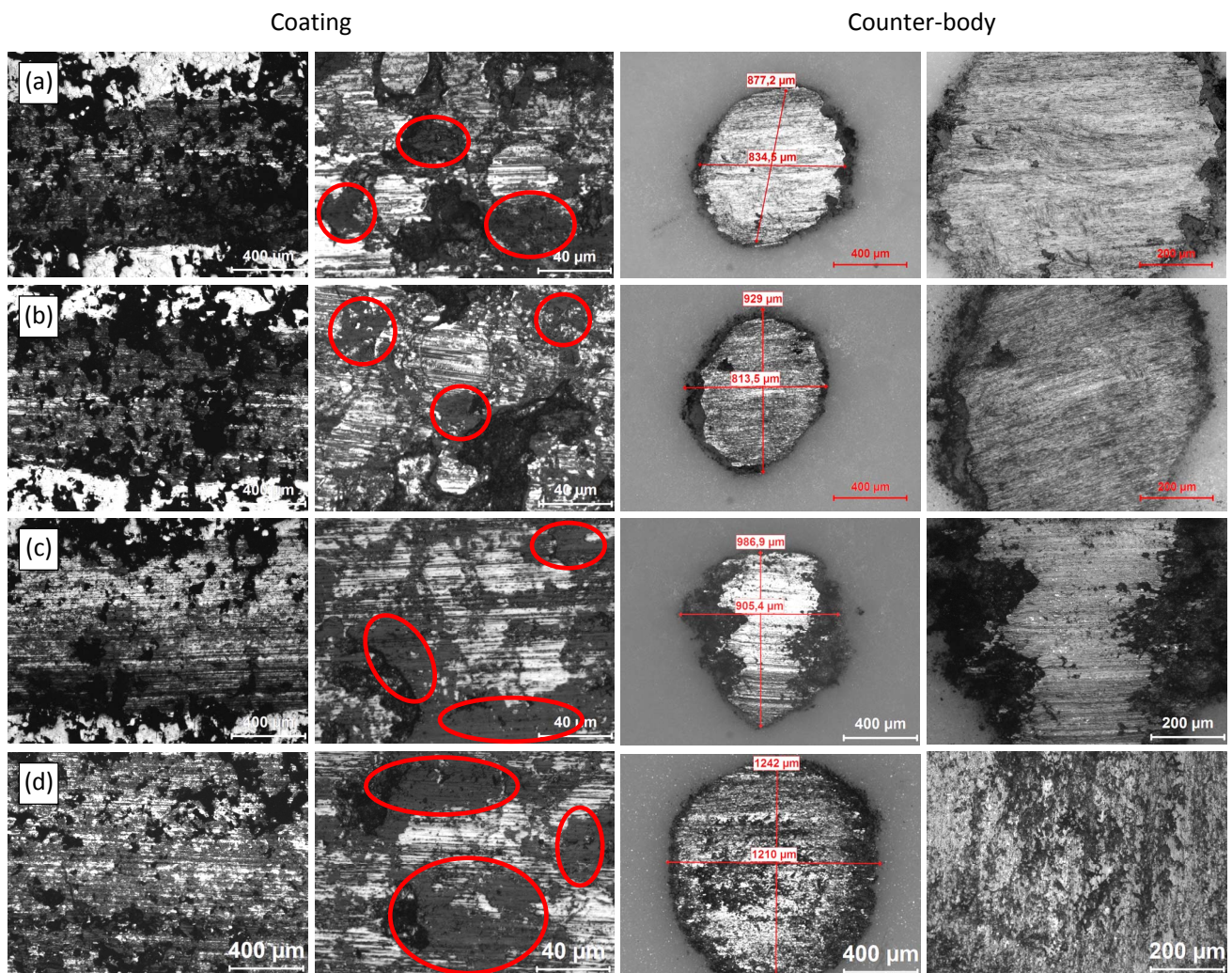


**Figure 4.** Lower (50x) and higher (100x) magnification LOM images of the wear tracks of coating and Al<sub>2</sub>O<sub>3</sub> ball sliding on coating: (a) 316L plasma nitrided at 450 °C, (b) 316L plasma nitrided at 500 °C, (c) 420 plasma nitrided at 450 °C and (d) 420 plasma nitrided at 500 °C

**Table 4.** Total wear values

Coating	Plasma nitriding temperature, °C	Wear track width, $\mu\text{m}$	Wear track depth, $\mu\text{m}$	Wear volume, $\text{mm}^3$	Specific wear rate $\times 10^{-5}$ , $\text{mm}^3/\text{Nm}$
316L	–	1790	52.6	0.820	47.55
	450	770	8.4	0.059	3.43
	500	731	14.2	0.078	4.55
420	–	2390	106.0	2.128	123.38
	450	890	16.0	0.116	6.71
	500	1180	12.0	0.161	9.31

Analysis of the plasma nitriding temperatures reveals that the wear volume and specific wear rate increase with higher temperatures for both coatings. A comprehensive comparison of all wear microscope images shows that the lowest specific wear rate and wear volume occur in the HVOF sprayed 316L and 420 coatings plasma nitrided at 450 °C. HVOF sprayed coatings plasma nitrided at 450 °C with a larger case depth (Fig. 3) demonstrated prominent resistance to deformation because the diffusion zone increased the compound zone's load-bearing capacity. Lastly, across all wear tests, it was determined that the substrate material remained undamaged and all tested coatings withstood a test load of up to 30 N without failure.

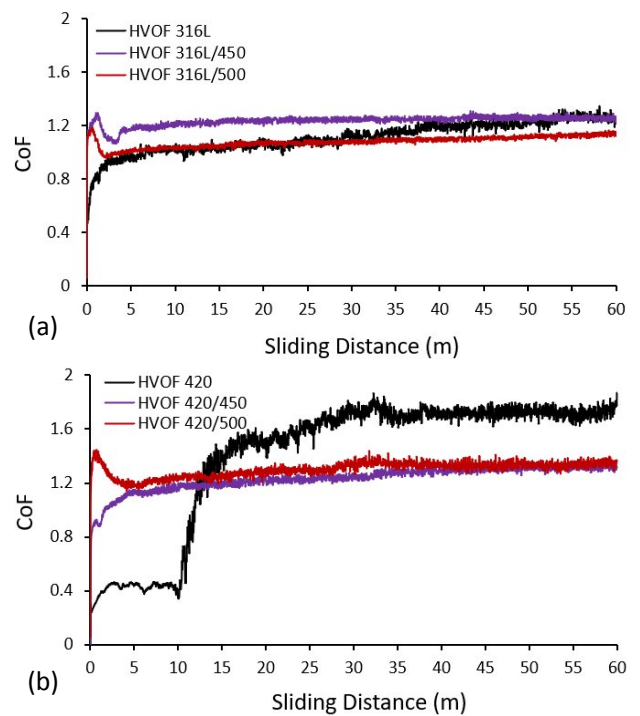
The values of the coefficient of friction provided in Figure 5 have been continuously recorded in a computer environment. The graphs show that the coefficient of friction of non-nitrided 316L coating increases with sliding distance and approaches a value of approximately 1.22. On the other hand, 316L coatings plasma nitrided at 450 and 500 °C exhibit stable friction with minor fluctuations (Fig. 5a). The coefficient of friction of non-nitrided 420 coating is initially 0.4 over the first 10 m and then rises to the value of 1.72 with increased fluctuations. In contrast, 420 coatings plasma nitrided at 450 and 500 °C maintain a stable coefficient of friction with lesser fluctuations (Fig. 5b). The nitriding process has led to a significant and favourable change in the coefficient of friction behaviour of both 316L and 420 coatings. Table 5 presents the calculated values of the steady-state coefficient of friction.

A Taguchi L4 orthogonal array design was conducted using the signal-to-noise (S/N) ratio "smaller-is-better" approach for the experiments since the lowest possible specific wear rate is desired [12]. Table 6 shows factors and their levels while Table 7 provides S/N ratios of specific wear rate results which are calculated using Equation 1.

Finally, the slopes of the factors in Figure 6 show the sole effect of factors on specific wear rates.

$$S/N_i = -10 \log_{10}(\mu_i^2 + \sigma_i^2), \quad (1)$$

where  $\mu$  is the average response (specific wear rate) and  $\sigma$  is the standard deviation in the response.

**Figure 5.** Evolution of the coefficient of friction with sliding distance for non-nitrided and plasma nitrided HVOF sprayed coatings: (a) 316L and (b) 420**Table 5.** Steady-state coefficient of friction values

Coating	Plasma nitriding temperature, °C	Coefficient of friction
316L	–	$1.22 \pm 0.039$
	450	$1.26 \pm 0.015$
	500	$1.11 \pm 0.018$
420	–	$1.72 \pm 0.034$
	450	$1.30 \pm 0.018$
	500	$1.33 \pm 0.021$

**Table 6.** Experimental design table

Factor	Level	
	+ 1	- 1
Coating material	316L	420
Plasma nitriding temperature	450 °C	500 °C

**Table 7.** Taguchi analysis results

Coating	Plasma nitriding temperature, °C	S/N ratio, dB
316L	450	- 10.68
	500	- 13.14
420	450	- 16.53
	500	- 19.74

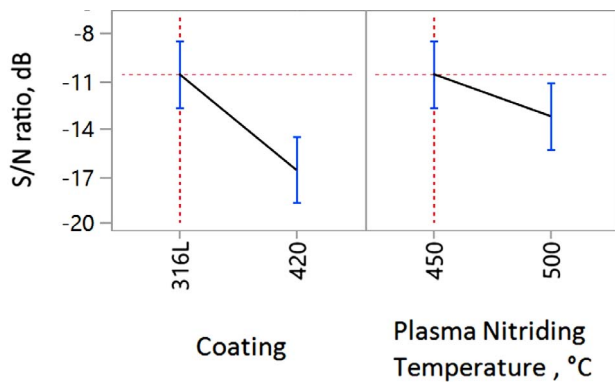


**Figure 6.** Taguchi analysis results

The prediction values for the specific wear rate were calculated using Equation 2 and given in Table 8. The error value was calculated by determining the difference between the model prediction and the experimental results and was presented in percentage. The model predicts fairly good approximations for specific wear rates. The maximum difference between the experimental results and the model was 10.82 %.

$$SWR = -11.675 \begin{cases} -2.015 & \text{for 316L} \\ 2.015 & \text{for 420} \end{cases} + 0.0372T, \quad (2)$$

where *SWR* is the specific wear rate in mm<sup>3</sup>/Nm and *T* is the plasma nitriding temperature in °C.

The analysis of variance (ANOVA) results for specific wear rates are shown in Table 9. ANOVA provides a second level of analysis which is useful for judging the statistical significance of the factor, which involves the study of the sources of variance in the data.

In Table 9, *SS* denotes the sum of squares for each factor and represents the variability of the

model. The expression of *SS* for a two-level column is given in Equation 3.

$$SS = n_{-1}(m_{-1} - m^*)^2 + n_{+1}(m_{+1} - m^*)^2, \quad (3)$$

where *m\** is the overall average for the specific wear rate and *m<sub>-1</sub>* and *m<sub>+1</sub>* are the average values of the specific wear rate for level -1 or +1, respectively; similarly, *n<sub>-1</sub>* and *n<sub>+1</sub>* are the number of specific wear rate experiments for each factor, which is two in this study, with a level of -1 or +1, respectively.

**Table 8.** Model prediction and comparison with experimental results

Coating	316L		420	
	450	500	450	500
Plasma nitriding temperature, °C				
Prediction for specific wear rate × 10 <sup>-5</sup> , mm <sup>3</sup> /Nm	3.05	4.91	7.08	8.94
Experimental vs. model prediction difference, %	10.82	8.15	5.51	3.97

**Table 9.** ANOVA table for specific wear rate results with percentage contribution of each factor

Factor	SS	DOF	MS	F	%
Coating material	36.55	1	36.55	991.8	83.85
Plasma nitriding temperature	7.04	1	7.04	190.9	16.14
Error estimate	0.04	1	0.04	-	0.01

DOF stands for the degree of freedom of each row. Since full factorial design is selected in this study, each factor has one DOF representing the sole effect of the factor without any confounding in data.

MS denotes the mean square for the factors and is obtained by dividing the *SS* by the DOF value for each row. Since all factors and estimated errors have only one DOF, *SS* values are transferred to the MS column in this study. The expression of MS for each factor is given in Equation 4.

$$MS = \frac{SS}{DOF}. \quad (4)$$

In essence, a term equal to the mean square for the factors is divided by a similar term estimated for error to obtain an *F* value. The expression of *F* for each factor is given in Equation 5.

$$F = \frac{MS_{\text{factor}}}{MS_{\text{error}}} \quad (5)$$

A large value of F indicates a variance much larger than that anticipated from the error estimate. Calculated F values for each factor are compared with the F critical value which assists us in understanding whether a factor is statistically significant or not. In this study, the critical F value at a 95 % confidence level, with one degree of freedom and one error column was selected from the Funkenbusch as 161.45 [19]. It is noticed that the coating material is the most important factor contributing approximately 84 %, while plasma nitriding temperature is also an influential factor with a contribution of 16 %, being slightly higher than F critical for specific wear rate results.

The optimal configuration for a low specific wear rate was identified as HVOF sprayed 316L coating plasma nitrided at 450 °C. Analysis of the specific wear rate values from Table 4, along with the worn surfaces of coatings and counter-bodies shown in Figure 7, revealed that different coating materials significantly affected the wear rate. Notably, the 316L coating had a wear rate approximately three times lower than that of the 420 coating. Since the HVOF sprayed stainless steel coatings used for this study were stacked with melted particles and hard oxide layers (Fig. 2), they exhibited a lower wear rate than the bulk stainless steel, which had very similar values ( $125.89 \times 10^{-5} - 133.9 \times 10^{-5} \text{ mm}^3/\text{Nm}$ ) as shown in Dalmau et al. [20]. However, it is important to emphasise that plasma nitriding is still an important factor, as the layers formed on the

surface after plasma nitriding enhance the coating's wear resistance.

#### 4. Conclusion

Two different coating materials, AISI 316L and AISI 420, were applied to low-carbon steel using the HVOF method. Subsequently, these coatings were subjected to plasma nitriding processes at two different temperatures (450 and 500 °C) to primarily investigate the variations in specific wear rates of the coatings. The results can be summarised as follows:

- HVOF sprayed 316L coating is more resistant to wear compared to 420 coating.
- Plasma nitriding at 450 °C yields better results in terms of wear resistance compared to the process applied at 500 °C.
- Based on the analysis of the results obtained with the statistical tools, the optimal configuration is HVOF sprayed 316L coating plasma nitrided at 450 °C.
- Statistical analysis identified coating material as the most important factor. Additionally, plasma nitriding is also an influential factor by a small margin. The statistical model predicts fairly good results in comparison to the experimental one, having the highest error of 10.82 %.

Future work will aim to enhance the statistical analysis and experimental design by increasing the number of parameters and responses. The goal is to apply multivariable optimisation using statistical analysis for multiple responses such as coefficient of friction, hardness, surface roughness and others.

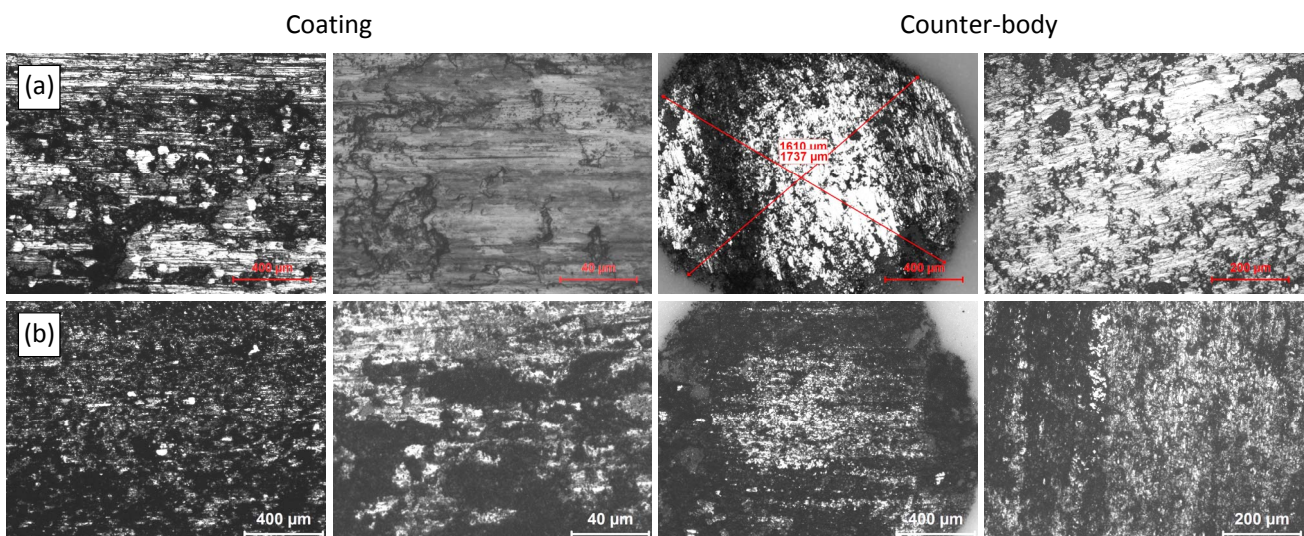


**Figure 7.** Lower (50x) and higher (100x) magnification LOM images of the wear tracks of coating and  $\text{Al}_2\text{O}_3$  ball sliding on coating: (a) 316L and (d) 420

## Acknowledgement

This study was supported by the research foundation of Bilecik Şeyh Edebali University (Project No. 2023-01.BŞEÜ.03-02). We also extend our gratitude to Dr. Ersin E. Korkmaz for applying the plasma nitriding treatment to the steels.

## References

- [1] A. Vencl, S. Arostegui, G. Favaro, F. Zivic, M. Mrdak, S. Mitrović, V. Popovic, Evaluation of adhesion/cohesion bond strength of the thick plasma spray coatings by scratch testing on coatings cross-sections, *Tribology International*, Vol. 44, No. 11, 2011, pp. 1281-1288, DOI: [10.1016/j.triboint.2011.04.002](https://doi.org/10.1016/j.triboint.2011.04.002)
- [2] W. Tillmann, L. Hagen, C. Schaak, J. Liß, M. Schaper, K.-P. Hoyer, M.E. Aydinöz, K.-U. Garthe, Adhesion of HVOF-sprayed WC-Co coatings on 316L substrates processed by SLM, *Journal of Thermal Spray Technology*, Vol. 29, No. 6, 2020, pp. 1396-1409, DOI: [10.1007/s11666-020-01081-y](https://doi.org/10.1007/s11666-020-01081-y)
- [3] R.F. Vaz, V. Luzin, F. Salvemini, G.G. Ribamar, J.A. Ávila, V. Albaladejo, J. Sanchez, I.G. Cano, The effect of the deposition strategy and heat treatment on cold spray additive manufactured 316L stainless steel, *Advanced Engineering Materials*, Vol. 26, No. 14, 2024, Paper 2302156, DOI: [10.1002/adem.202302156](https://doi.org/10.1002/adem.202302156)
- [4] J. Daniel, Š. Houdková, J. Duliškovič, J. Grossman, Impact wear of the Co-based HVOF-sprayed coatings, *Tribology International*, Vol. 187, 2023, Paper 108755, DOI: [10.1016/j.triboint.2023.108755](https://doi.org/10.1016/j.triboint.2023.108755)
- [5] R.F. Vaz, A.G.M. Pukasiewicz, H.D.C. Fals, L.A. Lourençato, R.S.C. Paredes, Study of particle properties of different steels sprayed by arc spray process, *Coatings*, Vol. 10, No. 4, 2020, Paper 417, DOI: [10.3390/coatings10040417](https://doi.org/10.3390/coatings10040417)
- [6] K. Bobzin, L. Zhao, M. Öte, T. Königstein, M. Steeger, Impact wear of an HVOF-sprayed Cr<sub>3</sub>C<sub>2</sub>-NiCr coating, *International Journal of Refractory Metals and Hard Materials*, Vol. 70, 2018, pp. 191-196, DOI: [10.1016/j.ijrmhm.2017.10.011](https://doi.org/10.1016/j.ijrmhm.2017.10.011)
- [7] G. Park, G. Bae, K. Moon, C. Lee, Effect of plasma nitriding and nitrocarburizing on HVOF-sprayed stainless steel coatings, *Journal of Thermal Spray Technology*, Vol. 22, No. 8, 2013, pp. 1366-1373, DOI: [10.1007/s11666-013-0035-4](https://doi.org/10.1007/s11666-013-0035-4)
- [8] A. Sagalovych, V. Sagalovych, V. Popov, S. Dudnik, O. Olijnyk, Tribological characteristics of samples made from titanium alloy VT5 nitrided in plasma glow discharge, *Tribology and Materials*, Vol. 1, No. 3, 2022, pp. 106-113, DOI: [10.46793/tribomat.2022.013](https://doi.org/10.46793/tribomat.2022.013)
- [9] S. Adachi, N. Ueda, Wear and corrosion properties of cold-sprayed AISI 316L coatings treated by combined plasma carburizing and nitriding at low temperature, *Coatings*, Vol. 8, No. 12, 2018, Paper 456, DOI: [10.3390/coatings8120456](https://doi.org/10.3390/coatings8120456)
- [10] J. Li, X. Tao, W. Wu, G. Xie, Y. Yang, X. Zhou, S. Zhang, Effect of arc current on the microstructure, tribological and corrosion performances of AISI 420 martensitic stainless steel treated by arc discharge plasma nitriding, *Journal of Materials Science*, Vol. 58, No. 5, 2023, pp. 2294-2309, DOI: [10.1007/s10853-023-08161-8](https://doi.org/10.1007/s10853-023-08161-8)
- [11] A.M. Hebbale, M.S. Srinath, Taguchi analysis on erosive wear behavior of cobalt based microwave cladding on stainless steel AISI-420, *Measurement*, Vol. 99, 2017, pp. 98-107, DOI: [10.1016/j.measurement.2016.12.024](https://doi.org/10.1016/j.measurement.2016.12.024)
- [12] O. Hussain, S.S. Saleem, B. Ahmad, Friction and wear performance evaluation of UHMWPE using Taguchi based grey approach: A study on the influence of load and bio-serum lubrication, *Materials Chemistry and Physics*, Vol. 239, 2020, Paper 121918, DOI: [10.1016/j.matchemphys.2019.121918](https://doi.org/10.1016/j.matchemphys.2019.121918)
- [13] H. Mindivan, Wear behavior of plasma and HVOF sprayed WC-12Co + 6% ETFE coatings on AA2024-T6 aluminum alloy, *Surface and Coatings Technology*, Vol. 204, No. 12-13, 2010, pp. 1870-1874, DOI: [10.1016/j.surfcoat.2009.10.050](https://doi.org/10.1016/j.surfcoat.2009.10.050)
- [14] *Thermal Spray Materials Guide*, Oerlikon Metco, Westbury, 2015.
- [15] H. Mindivan, Pulsed plasma nitriding of high velocity oxy-fuel sprayed Inconel 625 coatings, *Proceedings of the Institution of Mechanical Engineers, Part J: Journal of Engineering Tribology*, Vol. 236, No. 10, 2022, pp. 1950-1961, DOI: [10.1177/13506501211062522](https://doi.org/10.1177/13506501211062522)
- [16] B.S. Johnny, M. Alphonse, Friction and wear behaviour of AlCrN and TiN coated H13 tool steel, *Tribology and Materials*, Vol. 3, No. 3, 2024, pp. 131-140, DOI: [10.46793/tribomat.2024.015](https://doi.org/10.46793/tribomat.2024.015)
- [17] F. Mindivan, H. Mindivan, Surface properties and tribocorrosion behaviour of a thermal sprayed martensitic stainless steel coating after pulsed plasma nitriding process, *Advances in Materials and Processing Technologies*, Vol. 2, No. 4, 2016, pp. 514-526, DOI: [10.1080/2374068X.2016.1247232](https://doi.org/10.1080/2374068X.2016.1247232)
- [18] Y.-x. Peng, X.-d. Chang, S.-s. Sun, Z.-c. Zhu, X.-s. Gong, S.-y. Zou, W.-x. Xu, Z.-T. Mi, The friction and wear properties of steel wire rope sliding against itself under impact load, *Wear*, Vol. 400-401, 2018, pp. 194-206, DOI: [10.1016/j.wear.2018.01.010](https://doi.org/10.1016/j.wear.2018.01.010)
- [19] P.D. Funkenbusch, *Practical Guide To Designed Experiments*, CRC Press, Boca Raton, 2004, DOI: [10.4324/9780203997314](https://doi.org/10.4324/9780203997314)

[20] A. Dalmau, W. Rmili, D. Joly, C. Richard, A. Igual-Muñoz, Tribological behavior of new martensitic stainless steels using scratch and

dry wear test, Tribology Letters, Vol. 56, No. 3, 2014, pp. 517-529, DOI: [10.1007/s11249-014-0429-6](https://doi.org/10.1007/s11249-014-0429-6)